

25

INSTITUTE FOR NUCLEAR STUDY  
UNIVERSITY OF TOKYO  
Tanashi, Tokyo 188  
Japan

INS-Rep. -1099  
May 1995

## High resolution TOF detector

for hypernuclear lifetime measurement

Y.D. Kim<sup>b,c</sup>, H. Bhang<sup>a</sup>, O. Hashimoto<sup>b</sup>, K. Maeda<sup>d</sup>, K. Omata<sup>b</sup>,

H. Oota<sup>b</sup>, H. Park<sup>a</sup>, M. Yunn<sup>a,b</sup>

<sup>a</sup> *Department of Physics, Seoul National University, Seoul 151-742, Korea*

<sup>b</sup> *Institute for Nuclear Study (INS), University of Tokyo, Tanashi, Tokyo 188, Japan*

<sup>c</sup> *National Laboratory for High Energy Physics (KEK), Oho, Tsukuba, Ibaraki 305, Japan*

<sup>d</sup> *Department of Physics, Tohoku University, Kawauchi, Sendai, Miyagi 980-77, Japan*



SW 9525

*Submitted to Nuclear Instruments and Methods*

# High resolution TOF detector for hypernuclear lifetime measurement

Y.D. Kim<sup>b,c</sup>, H. Bhang<sup>a</sup>, O. Hashimoto<sup>b</sup>, K. Maeda<sup>d</sup>, K. Omata<sup>b</sup>,  
H. Outa<sup>b</sup>, H. Park<sup>a</sup>, M. Youn<sup>a,b</sup>

<sup>a</sup> Department of Physics, Seoul National University, Seoul 151-742, Korea

<sup>b</sup> Institute for Nuclear Study(INS), University of Tokyo, Tanashi, Tokyo 188, Japan

<sup>c</sup> National Laboratory for High Energy Physics (KEK), Oho, Tsukuba, Ibaraki 305, Japan

<sup>d</sup> Department of Physics, Tohoku University, Kawauchi, Sendai, Miyagi 980-77, Japan

## Abstract

We have tested several types of TOF counters based on scintillator and photomultiplier tube in order to measure the lifetime of hypernuclei. With the advantage of small size of the counter, we obtained less than 30 ps of timing resolution, and about 50 ps of overall TOF resolution. The various factors in this resolution have been studied. The timing resolution dependence on the beam intensity is also studied.

## 1 Introduction

Recently we have seen reports on the measurement of lifetime of short-living hypernuclei [1, 2, 3] directly measuring the time difference between the formation and decay of hypernuclei. The lifetime of these measurements ranges from 194 ps to 256 ps with about 15 % measurement errors. These experiments used scintillating Time of Flight(TOF) detectors, and the errors were small compared to the previous measurements using other detectors such as emulsion or bubble chambers.

The statistical error in the measurement of hypernuclei lifetime is approximately  $\sqrt{\frac{\tau^2 + \sigma^2}{N}}$ . Here  $\tau$  is the lifetime of hypernuclei itself,  $\sigma$  is the resolution of TOF counters, and  $N$  is the number of hypernuclei events measured. If  $N$  is 200 and  $\sigma \approx \tau$ , then the error would be about 10 % of the obtained lifetime  $\tau$ . Therefore the minimum lifetime measurable with about 10 % resolution is the same as  $\sigma$  when the number of events is about 200. The more sophisticated analysis using maximum likelihood fitting method is expected to give a little smaller error than this value[1].

We would like to measure the lifetime with about 10 % of total error for a rather wide time range over 100 ps. Recently timing resolutions of scintillating counters better than 100 ps have been reported mainly due to the development in photomultiplier tubes(PMT) and scintillator technology [4, 5]. Our TOF system consists of two parts ; beam timing counter and decayed-particle timing counter. We plan to use 1.05 GeV pion (minimum ionizing particles), and the particles from hypernuclei decay will be pions and protons with kinetic energy of 40-120 MeV(non-minimum ionizing particles).

Considering the geometry of our experiment, we can use small size( $< 20cm$ ) scintillators, which is important factor to achieve less than 100 ps TOF resolution. However, most of the previous measurements on the timing resolution were for large size scintillators and at low particle count rate. In this report, we describe our test experiments on the timing resolution for small size(less than 20cm length) scintillators at both low and high count rate. The experimental setup is described in section 2, and the analysis method of the data is explained in section 3. In section 4 we present our results at low rate of the beam, and the high rate results will be presented in section 5.

## 2 Setup of test

The test experiment was performed at T1 test beam line at KEK. Figure 1 shows the test setup. The magnet was set to select positive charged particles with the momentum of 500 MeV/c. The kinetic energies of pions and protons are 380 and 125 MeV respectively. The beam go through start(S) counter( $1 \times 1.5 \times 1 \text{ cm}^3$ ), two counters to be tested, and defining(D)( $2 \times 2 \times 1.5 \text{ cm}^3$ ) counter successively. To identify the particles, we located two large size scintillation counter before the start counter(P1) and after the defining counter(P2) with flight length of 2.5 m. The pion and proton were separated without any background with the difference in the time of flight between these two counters. From the previous measurement using this test beam line, it is known that there are comparable number of positrons as well as pions. So our pion beam data include these electrons.

We prepared several prototype counters schematically drawn in figure 2. The specifications of each counter we tested are listed in table 1. We tested B1 and B2 types for beam counter(smaller size) and D types for decay counter(larger size but still  $4 \text{ cm} \times 16 \text{ cm}$ ). Table 2 contains the specifications of two different types of Hamamatsu PMTs. The criteria to select the optimal PMT type we considered were the size, transit time spread(TTS) values, and rise times. TTS values referred in the Hamamatsu catalogue were for single photoelectron, and PMTs with smaller TTS values are selected.

We also tested two different scintillation materials supplied by Bicron, BC418 and BC420. The decay constants for BC418 and BC420 are 1.4 and 1.5 ns respectively, the shortest ones of Bicron products at the time of test. The bulk attenuation lengths of these are 100 and 110 cm respectively. These are much shorter than the commonly used BC408 scintillators. However, for small size scintillators, the bulk attenuation length should not be a big effect. The light guides were made by ultra violet (UV) lucite, and attached to the scintillators and PMTs with optical cement (NE-581). For D type counter, we tested two different shapes of light guides, Fish-tail and Twisted shapes. The twisted one was divided into 3 leaves to be matched to the size of R3478 photocathode(15mm in diameter).

One of two anode signals of each tested PMTs were connected to the leading-edge discriminator(Philips 710). The cable length between PMT and discriminator was  $\approx 3m$  to reduce the deterioration of rising part of the PMT signal. The outputs of discriminator were connected to another discriminator once again before it enters

the TDC module after about 200 ns delay. A High Resolution(HR) TDC fabricated by KEK, with 25ps per channel resolution was used. For the trigger, coincidence between the start(S) and defining(D) counters was required, and the time '0' signal of the HR TDC was given by start(S) counter. The ADC and TDC signals for all PMTs were recorded by a personal computer using KODAQ data acquisition software.[13] The single rate on the counters tested was less than 10,000/sec, and the trigger rate was about 100/sec for the low count rate test.

### 3 Analysis

The timing resolution of each counter was obtained by solving the three linear equations of the three TOF resolutions between start and two test counters;  $\sigma(T_S - T_1)$ ,  $\sigma(T_S - T_2)$ , and  $\sigma(T_1 - T_2)$ . Here  $T_i$  is the mean time of two PMTs for each counter. First pions and protons are separated with the TOF spectra between P1 and P2 counters. And we selected the events which had the correct pulse height on the start(S) counter by putting a cut of one  $\sigma$  width on the ADC spectra around the centroid of each pion or proton to reduce the error in the estimation of  $\sigma(T_1)$  and  $\sigma(T_2)$ . This cut didn't affect the values of  $\sigma(T_1)$  and  $\sigma(T_2)$  itself. Then we obtained the standard deviations ( $\sigma$ ) of the three TOF distributions. Figure 3 shows the typical timing spectra of a B1 type counter(15mm thickness) obtained with pions. Two test counters were identical in specifications. Figure 3(a) shows a 2 dimensional scatter plot of geometrical mean of pulse heights of one TEST counter versus TOF timing between two TEST counters. The one-dimensional TOF distribution between two TEST counters is shown in Figure 3(c) with the standard deviation of 65 ps without the pulse height correction.

It is known that the timing from the leading edge discriminator has a dependence on the pulse height of the signal according to the equation [7];

$$t' = t + \alpha \left( \frac{1}{\sqrt{q}} - \frac{1}{\sqrt{q_0}} \right) \quad (1)$$

here  $t'$  is the corrected time,  $t$  is the uncorrected time,  $\alpha$  is the correction coefficient,  $q$  is the height of the signal, and  $q_0$  is the reference pulse height. The correction was done for each PMT of the TEST counters;

$$(t_{iL} - t_S)' = t_{iL} - t_S + \alpha_{iL} \left( \frac{1}{\sqrt{q_{iL}}} - \frac{1}{\sqrt{q_{iL0}}} \right) \quad (2)$$

$$(t_{iR} - t_S)' = t_{iR} - t_S + \alpha_{iR} \left( \frac{1}{\sqrt{q_{iR}}} - \frac{1}{\sqrt{q_{iR0}}} \right) \quad (3)$$

$$t_i' - t_S = ((t_{iL} - t_S)' + (t_{iR} - t_S)')/2, i = 1, 2 \quad (4)$$

Figure 3(b),(d) show 2 dimensional scatter plot and 1-D TOF distribution after this pulse height correction. The data points in Figure 3(d) are binned with 0.1 ch after the correction to minimize the binning effect on the resolution. After the correction we obtained 40 ps of TOF resolution, which means 28 ps(!) timing resolution for each counter. We also tried to correct  $t_1 - t_2$  using geometrical mean of the signal height and the results were consistent with those after correction on each PMTs within 3ps.

Since each counter has two PMTs in equal condition to collect photons with the beam in the center of the counter, it is possible to estimate the number of photoelectrons from the statistical fluctuations in the counting[8]. If  $R$  is the pulse height of one PMT and  $L$  is that of the other PMT, then

$$\delta = \frac{R - L}{R + L}, \quad \sigma_\delta = \frac{1}{\sqrt{N_{p.e.}}} \quad (5)$$

Here  $N_{p.e.}$  is the sum of the number of photoelectrons in both of PMTs. The validity of this equation is based on the fact that the relative gains in two PMTs are matched and the average number of photoelectrons in two PMTs are equal. Practically there are two more sources contributing to  $\sigma_{\delta, measured}$ . First the finite size of the beam on the counter would increase  $\sigma_{\delta, measured}$  due to the difference in photon collection efficiency( $\sigma_{\delta, b}$ ). If the beam size is  $b$ , and the attenuation length is  $\lambda$ , then  $\sigma_{\delta, b} = \frac{1}{\sqrt{12}} \frac{b}{\lambda}$ . In our test experiment  $b = 1$  cm, which is the size of start(S) counter. To estimate the attenuation length,  $\lambda$ , and investigate timing resolution at different hit positions, we moved one counter along the perpendicular direction to the beam by 2cm steps. A D type counter of BC420 with 6 mm thickness was tested. In Figure 4, the pulse height of a PMT signal has been plotted as a function of hit positions. The two fitted exponential lines are for pions and protons. The extracted attenuation length was about 50cm for both cases, which is about factor of 2 smaller than the bulk attenuation length of the scintillator. Consequently  $\sigma_{\delta, b} \approx 0.006$ , which is negligible for smaller(a few hundreds) number of photoelectrons extracted. For 2000 photoelectrons, its contribution is about 8 %. Secondly the fluctuations in PMT multiplication of single photoelectron and electronics noise also should contribute to  $\sigma_\delta(\sigma_{\delta, e})$ . Therefore,

$$\sigma_\delta^2 = \sigma_{\delta, measured}^2 - \sigma_{\delta, b}^2 - \sigma_{\delta, e}^2. \quad (6)$$

For more than 100 photoelectrons  $\sigma_{\delta, e}$  is negligible, so only  $\sigma_{\delta, b}$  was considered in our estimation. The extracted  $N_{p.e.}$  and its relation with timing resolution are described in next subsections.

### 4 Results

The timing resolution of long scintillating counters were reported at the range of 100-150 ps [9, 10]. The timing resolution of a long scintillating bar counter can be formulated empirically [10] ;

$$\sigma = a \sqrt{L/N_{p.e.}} \quad (7)$$

Here  $L$  is the length of the bar, and  $N_{p.e.}$  is the average number of photoelectrons collected. It is interesting to investigate the validity of this formula for small  $L$  or large  $N_{p.e.}$ , since one naturally expect a limitation at certain values of  $L$  or  $N_{p.e.}$ . For short scintillating counter, the timing resolution may be limited by other factors such as scintillator decay timing or PMT characteristics. It should be important to know which factor is dominant for the timing resolution for small size scintillating counters in order to optimize the resolution.

#### 4.1 Scintillating material dependence

BC418 and BC420 were selected for the test because of their short rising time. There was a report showing the effect of scintillation rising time on the timing resolution by comparing BC-408 and BC-420 [10]. We compared only BC-418 and BC-420 to see if there is any difference between two materials. The comparison was done for type D counters(6mm) with fish-tail light guides. After the pulse height correction, the timing resolutions of minimum ionizing particles (pion) were 59 ps and 55 ps for BC-418 and BC-420 respectively. Therefore there was not noticeable difference between two materials.

#### 4.2 Wrapping and light guide dependence

We also examined if the timing resolution depends on the wrapping materials due to the difference in the light collection efficiency. The three materials we tested were aluminum foil, aluminized mylar and black paper with same fish-tail light guides for type D counters. Aluminum foil and aluminized mylar were wrapped both on the scintillators and light guides, and black paper was wrapped only on the scintillator(light guide was wrapped with aluminum foil). Figure 5 shows the timing resolution of each counter as a function of  $N_{p.e.}$  extracted as described in section 3. The left 4 points are with pions and right 4 points are with protons. Even though there were noticeable differences in the pulse heights(black paper wrapping had 20 % smaller signal than aluminized-mylar wrapping), the timing resolutions were basically the same among the three cases. The filled square data point was for twisted light guide, which has largest number of photoelectrons collected. However there was no gain in the timing resolution. Conclusively, when the cross sections of scintillator and PMT window are fixed for small size scintillator, wrapping methods and light guide shapes didn't alter the timing resolution significantly.

#### 4.3 Discriminator threshold level dependence

The TOF resolution of scintillation counter may depend on the ratio between the discriminator threshold level and signal height. Figure 6 shows our test result on the timing resolution dependence on this variable. Only pions are selected, and the PMTs were R2083 tubes. The open(filled) circles are the resolutions without(with) pulse height correction. It shows that the timing resolution gets worse as the threshold level gets higher without pulse height correction. After the pulse height correction, the dependence disappeared if the  $\frac{V_{threshold}}{V_{signal}}$  is larger than 0.1. This is consistent with the behavior of the slewing correction coefficient, i.e., the slopes of the equation (1) is larger for the larger  $\frac{V_{threshold}}{V_{signal}}$  ratio, which is expected if one considers the shape of signal. This result indicates one can use rather lower high voltage safely when the anode current of a PMT is high due to high count rate.

#### 4.4 Position dependence

Figure 7 shows the TOF resolutions as a function of hit position along the length(16cm) of the scintillator(D type). The open circle data are the resolutions of each PMT, and the filled circle data are those of mean timing of two PMTs after ADC correction. The individual PMT resolution gets worse as the distance between the PMT and hit position gets larger due to the smaller number of photoelectrons collected, but the mean timing resolutions are constant over the full length within 3 ps.

#### 4.5 Number of photoelectrons dependence

In Figure 8, we plotted the timing resolutions of each counter as a function of  $\sqrt{\frac{L}{N_{p.e.}}}$  for both pions and protons. Here L is the distance between hit position and PMT window, basically length of scintillator and light guide, in units of cm. The resolutions measured with D type counters(4mm and 6mm, filled circles), B2 type counter(open circle), and one B1 type counter(filled square) are plotted. The light collection efficiency in the scintillator and light guide of D type counter is relatively low(about 10% estimated with Monte Carlo simulation program [12]) compared with the efficiency of B1 type counter (about 25%), which is fair agreement with the extracted number of photoelectrons. The solid line in the figure is a fit with a function of

$$\sigma = a\sqrt{\frac{L}{N_{p.e.}}} + b \quad (8)$$

The 'b' parameter of the fit was 10 ps, and 'a' value was 310. The fit indicates the empirical formula (7) is a fairly good approximation of timing resolution for the small size scintillators. Since the 'average length' of our counter is about 10cm, we can say that  $\sigma$  of one photoelectron is about 1ns. This value is in between the rise time and decay time of the scintillators we tested, and similar to the rise time of PMTs we tested(0.7ns for R2083 and 1.3ns for R3478). However it should be pointed out that the length parameter L is not a well defined parameter since it is the sum of scintillator and light guide for small size counters, therefore further detailed study may be needed for more quantitative arguments.

### 5 Rate dependence test

We tested the performance of our TOF counter in the high beam intensity, since the time '0' counter for lifetime should be located in the high intensity beam with about  $5 \times 10^6$  pions per second in our experiment. It is well known that PMT has non-linearity when the anode current becomes comparable to the bleeder current mainly due to the change in the voltage division ratio. The non-linearity in the gain can be overcome by supplying additional voltages through the last 3-4 dynode chains(booster voltage) [6]. More important and not well studied point is its timing behavior at high anode current. To test this, we located the counters with a similar setup shown in Figure 1 in the K5 beam line at KEK. Here we present the TOF results from only pions. We

tested two counters, B1 type(12 mm thickness, R2083) and B2 type(12 mm thickness, R3478) to compare different types of PMTs. For both PMTs we supplied additional voltages to last 3 dynode chains at the voltages measured without beam. The beam rate was estimated by the scaler counts of mean timer outputs of each test counter. Since the beam size was small enough to be inside of the test counter, the beam rates of two test counters were consistent within 10 %. We used CAEN HV power supplier for both main HV and bleeder chains. The maximum currents of this module was set at 3mA for each channel, and automatic recovering mode was used if it trips due to instant large current over the limit.

Figure 9 shows the pulse height variation as a function of pion rates. The open circles are the data without supplying booster voltage and the filled circles are with booster voltage supplied for R3478 PMT. As shown in the figure, the gain of R3478 PMT drops by about 30 % at 6 M/sec, while the booster voltage sustain the gain upto 5 M/sec with slight increase. In Figures 10 (a)(b), the timing resolution of each counter are shown as a function of pion rates for both R3478(a) and R2083 PMTs. For R3478 PMT the timing resolution gets much worse without booster voltages applied, more than 100 ps at the rate of 5 M pions/sec. The resolution with booster voltage applied was improved to be around 80 ps at the same rate. Similar deterioration of timing resolution is also observed in the case of R2083 PMT reaching around 60 ps at 5 M pions/sec as shown in the figure. On average, timing resolution gets worse upto factor of 2 for both PMTs even booster voltages applied.

Figure 11 shows ADC spectra of pions at low rate( $3 \times 10^4$  per second, hatched spectrum) (dotted line) and that at high rate( $5 \times 10^6$  per second) obtained with R3478 PMT. The width of the ADC spectrum at high rate is much broader than the one at low rate. Also the broadness directs towards larger ADC values, indicating signal pile-up. In figure 12, the correlation between timing resolution(x-axis) and ADC spectra width(y-axis) is shown. Again we can see the strong correlation between two values indicating that the two effects dependent on the rate are due to the same origin. It should be noted that we already excluded the events having explicitly two beam particles in the same potential beam microstructure from the ADC spectra for the data in figures 11 and 12. One possibility responsible for the deterioration in timing resolution is the pile-up between signals at high rate. Since the detail form of beam microstructure was not measured, it's difficult to estimate the quantitative effect of the pile-up on the timing resolution. At high rate, the PMT itself can be unstable, which could also contribute to the deterioration of timing resolution. It should be interesting to compare the effects with transistor based active base commonly used for gain stabilization.

## 6 Conclusion

We obtained very good timing resolutions with fast timing PMTs coupled to small size scintillator which can be used to measure the lifetime of hypernuclei larger than 100 ps. The timing resolutions of B1 type counter( $4 \times 6 \times 1.5 \text{ cm}^3$ ) and D type counter( $4 \times 1.6 \times 0.6 \text{ cm}^3$ ) with minimum ionizing particle were 29 ps and 59 ps respectively. For protons expected

from the hypernuclei non-mesonic decay, D type counter(6mm) had 36 ps resolution. Therefore the TOF resolution is expected to be 46 and 66 ps for protons and pions respectively. The timing resolution of each counter was not noticeably sensitive to the type of scintillator material, the method of wrapping, discriminator type and threshold level, and HV in the range we tested. The observed resolutions can be understood with the dependence on  $\sqrt{\frac{L}{N_{p.e}}}$  even for small size scintillators. At high rate, we observed the deterioration in the timing resolution by about factor of 2 for both PMT types. This effect has strong correlation with the broadening of pulse height width.

## Acknowledgements

We would like to thank the staff of KEK-PS for providing the beams in T1 and K5 area. The authors also wish to thank the staff of electron synchrotron laboratory of Tohoku University where we did a pre-test experiment to investigate the detector performance at high rate electron beam. Y.D. Kim and M. Youn acknowledges the financial support from JSPS postdoctoral fellowship program.

## References

- [1] R. Grace et. al., Phys. Rev. Lett. 55 (1985) 1055
- [2] J.J. Szymanski et al., Phys. Rev. C43 (1991) 849
- [3] H. Oota et al., Nucl. Phys. A547 (1992) 109c
- [4] T. Sugitate et al., Nucl. Instru. and Meth. A249 (1986) 354
- [5] T. Kobayashi et al., Nucl. Instru. and Meth. A287 (1990) 389
- [6] C. Ohmori et al., Nucl. Instru. and Meth. A256 (1987) 361
- [7] T. Tanimori et al., Nucl. Instru. and Meth. A216 (1983) 57
- [8] A. Andresen et al., Nucl. Instru. and Meth. A309 (1991) 101
- [9] V. Sum et al., Nucl. Instru. and Meth. A326 (1993) 489
- [10] S. Ahmad et al., Nucl. Instru. and Meth. A330 (1993) 416
- [11] H. Oota Ph.D. Thesis
- [12] D. Simon, GUIDEIT program.
- [13] For the reference, contact one of the author, K. Omata at INS.

Table 1: Specifications of the counters tested

Type	Size	PMT	Scintillator	Thickness	Light Guide	$\sigma_t(\pi)$
B1	4x6 cm <sup>2</sup>	R2083	BC418	0.8 cm	Disk 1.5cm	31 ps
				1.2	Disk 1.5cm	29
				1.5	Disk 1.5cm	28
B2	4x6	R3478	BC418	1.2	Fish-tail 5cm	41
D	4x16	R3478	BC418	0.4	Fish-tail 5cm	76
			BC420	0.6	Fish-tail 5cm	59
			BC418	0.6	Fish-tail 5cm	55
					Twisted 6cm	57

Table 2: Specifications of the PMTs tested

	R2083	R3478
photocathode size (D. mm)	46	15
rise time (ns)	0.7	1.3
transit time (ns)	16	14
TTS FWHM (ps)	370	360
gain	$2.5 \times 10^6$	$1.7 \times 10^6$
operational voltage(V)	3000	1700
No. of stages	8	8

## Figure Captions

Figure 1 : Experimental setup for beam tests at T1 beam line of KEK 12 GeV proton synchrotron.

Figure 2 : Details of counters tested. Thickness of each counters are listed in table 1. R2083 tubes were in hybrid type (H2431)

Figure 3 : (a) and (b) are the scatter plot of ADC versus TOF without and with the pulse height correction respectively. (c) and (d) are 1 dimensional plots of TOF showing the TOF resolutions in both cases.

Figure 4 : Attenuation length of a D type counter. The pulse heights of a PMT signal has been fitted exponentially as a function of hit positions.  $\lambda$  is about 50cm

- Figure 5 : Timing resolution as a function of  $N_{p.e}$ . The left 4 points are for pions and right 4 points for protons. TW means twisted light guide
- Figure 6 : The TOF resolution dependence on the discriminator threshold level for pions with B1 type counter(15mm thickness)
- Figure 7 : The TOF resolutions as a function of hit position along the length(16cm) of the scintillator. The data points are explained in the text.
- Figure 8 : The TOF resolution as a function of  $\sqrt{\frac{L(cm)}{N_{p.e}}}$ . Data from both pions and protons are plotted. The solid line in the figure is a fit with a function of  $\sigma = a\sqrt{\frac{L}{N_{p.e}}} + b$ .  $a=310$ ,  $b=11$  ps)
- Figure 9 : Pulse height(ADC value) versus beam rate, with(filled circles) and without(open circles) booster voltages applied.
- Figure 10 : The TOF resolutions versus beam rate, with(filled circles) and without(open circles) booster voltages applied.
- Figure 11 : ADC spectra at low and high beam rate
- Figure 12 : ADC width versus TOF timing resolution at the various beam rates as in Figure 10.

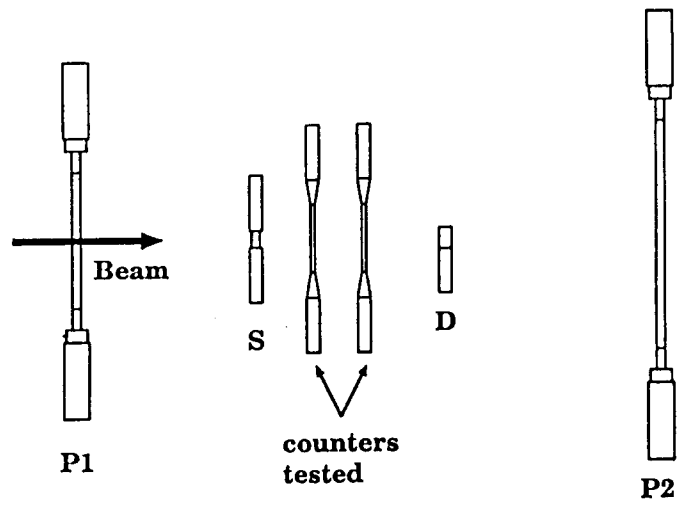


Fig. 1

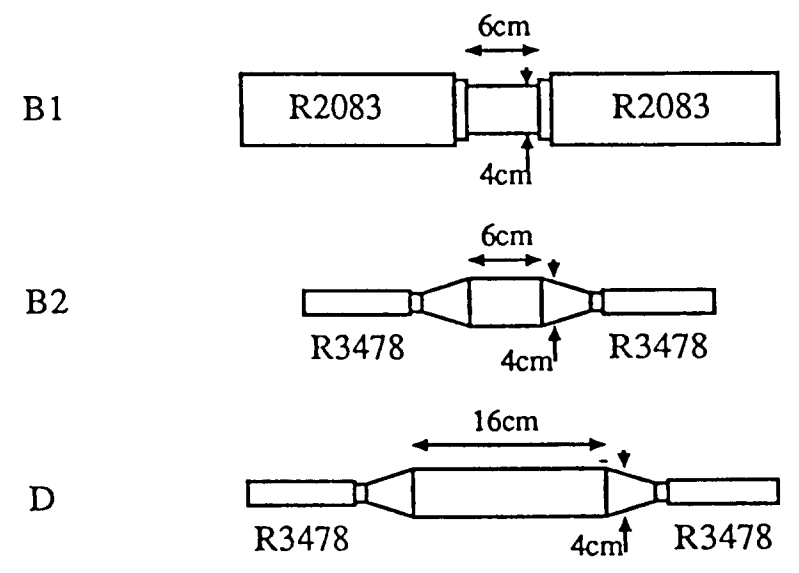


Fig. 2



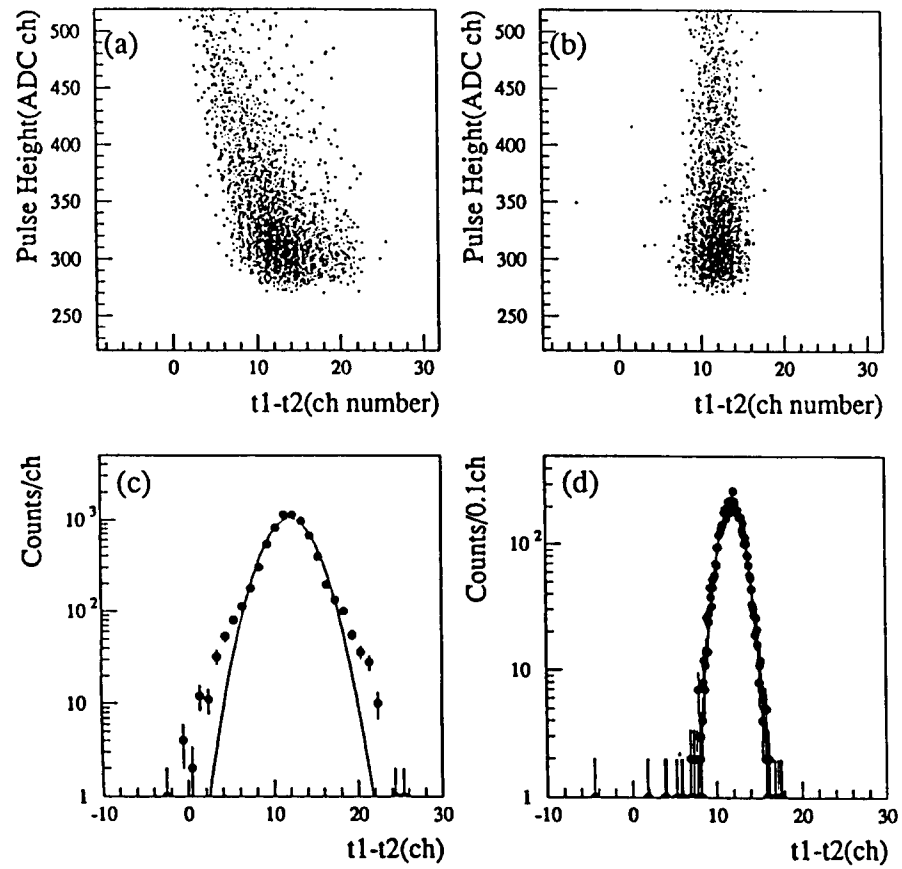


Fig. 3

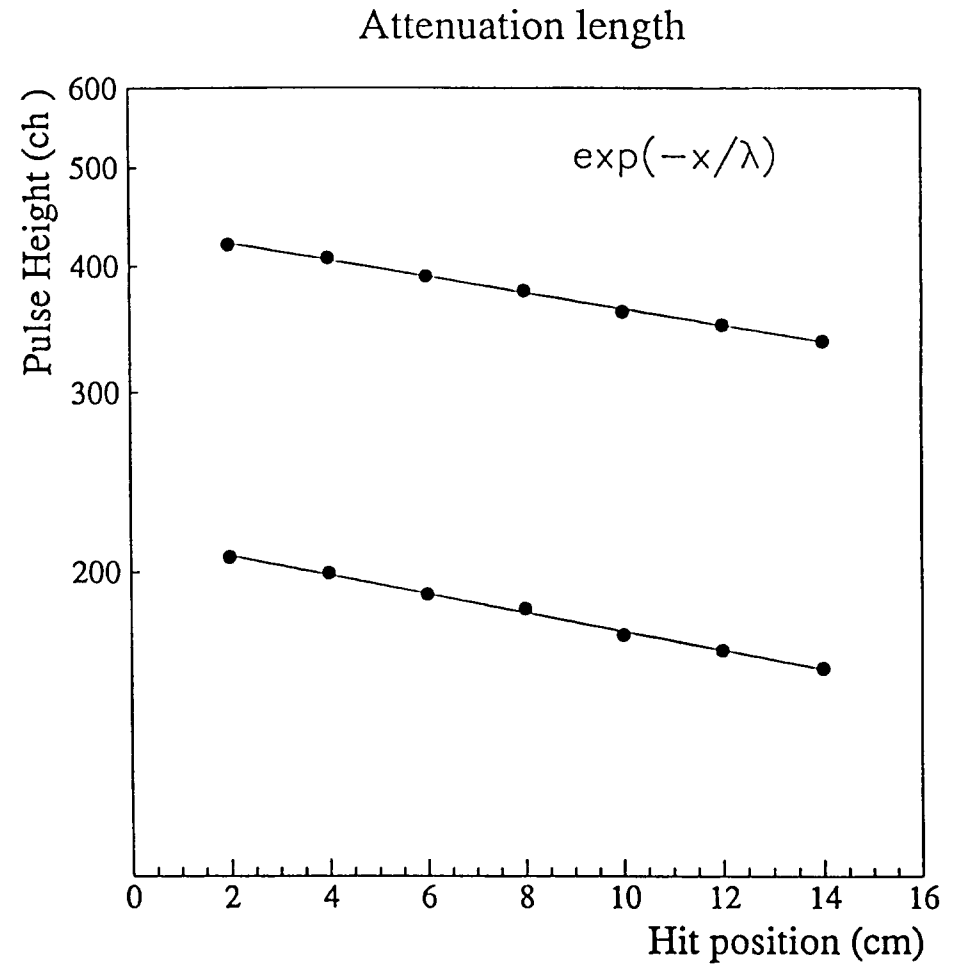


Fig. 4

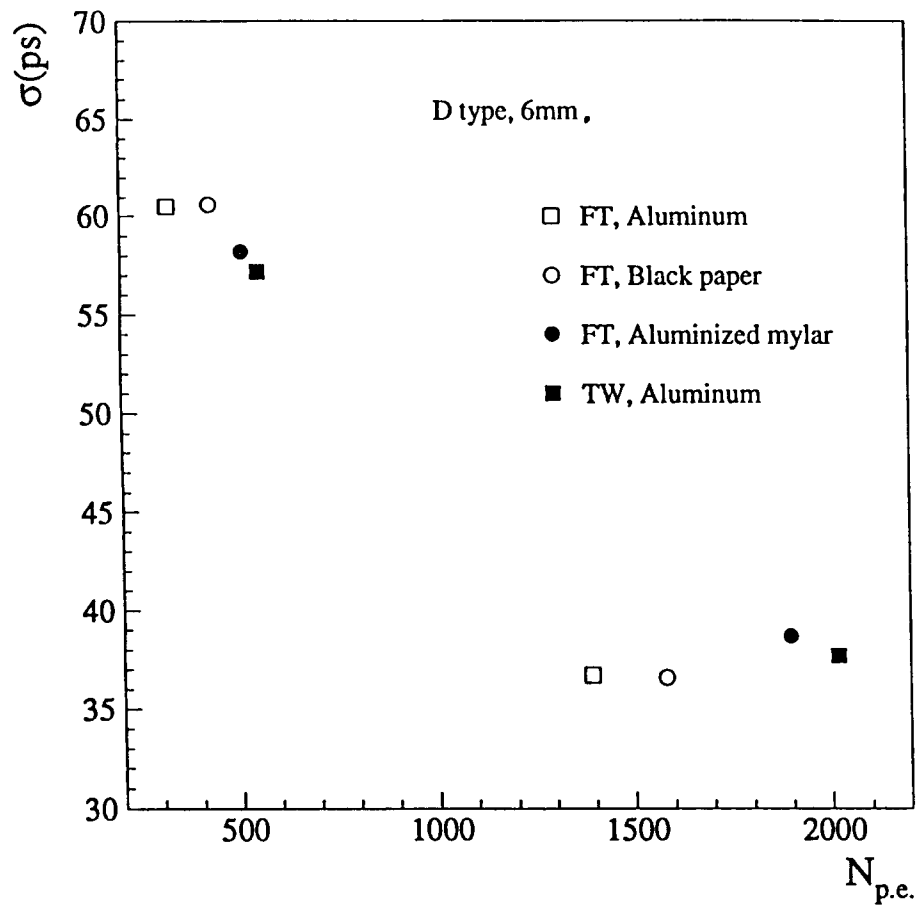


Fig. 5

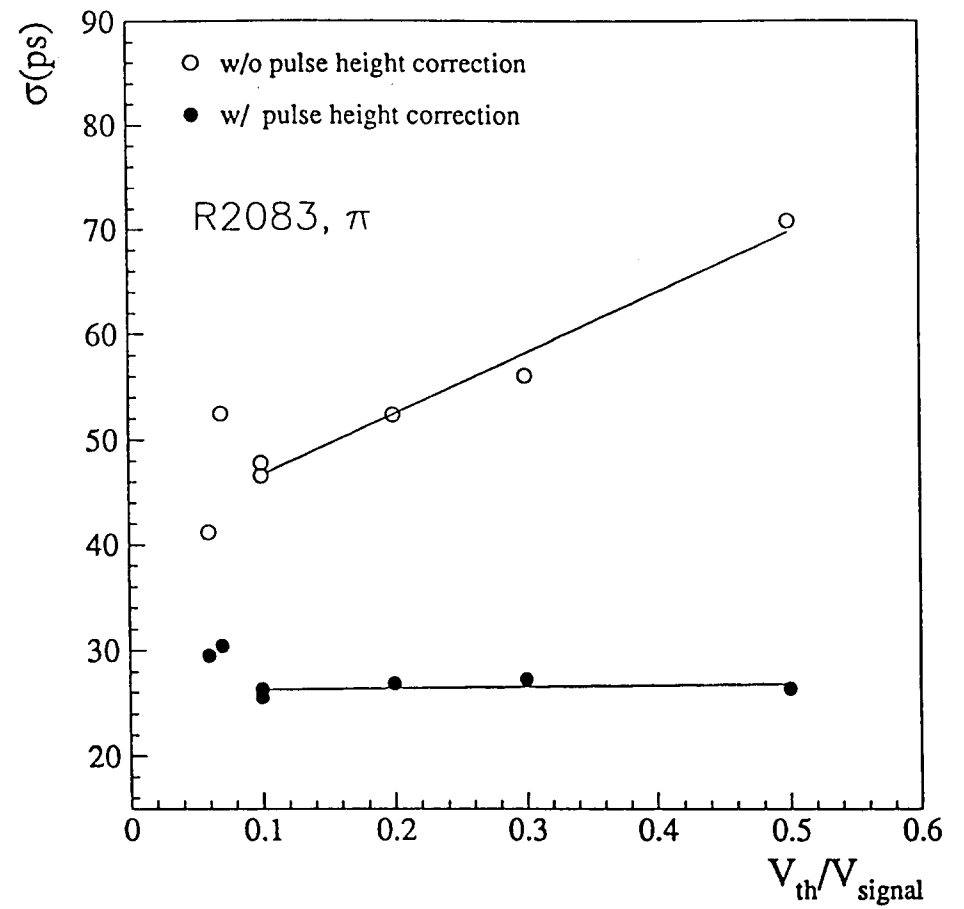


Fig. 6

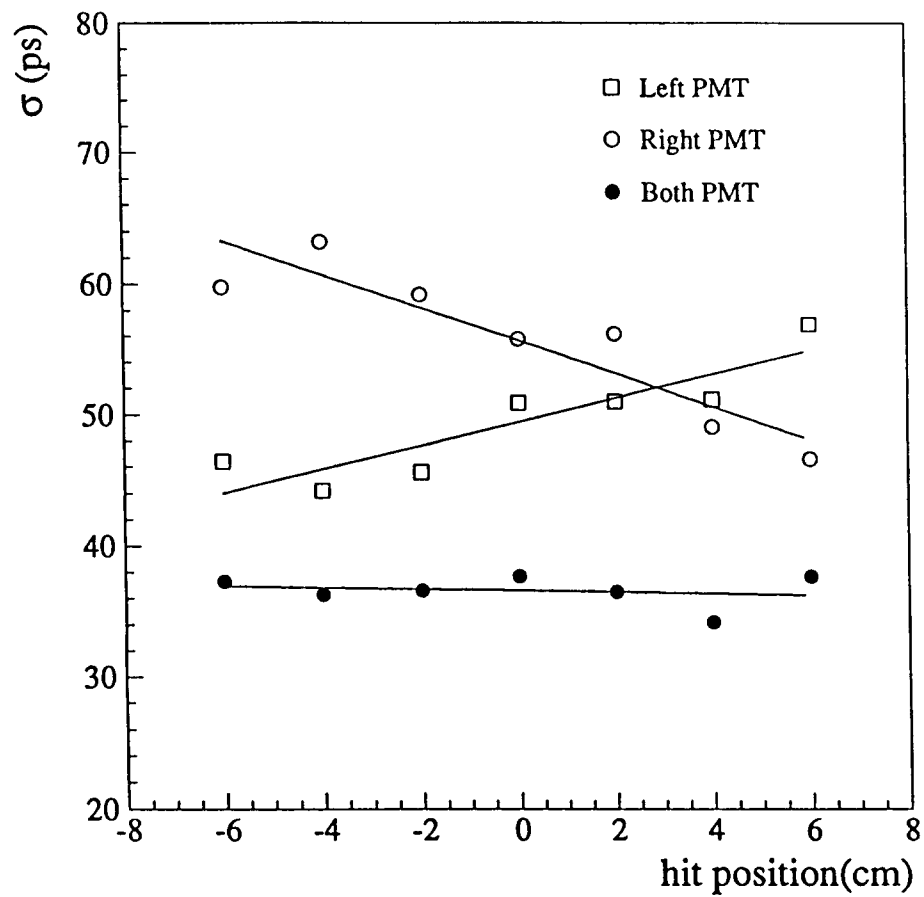


Fig. 7

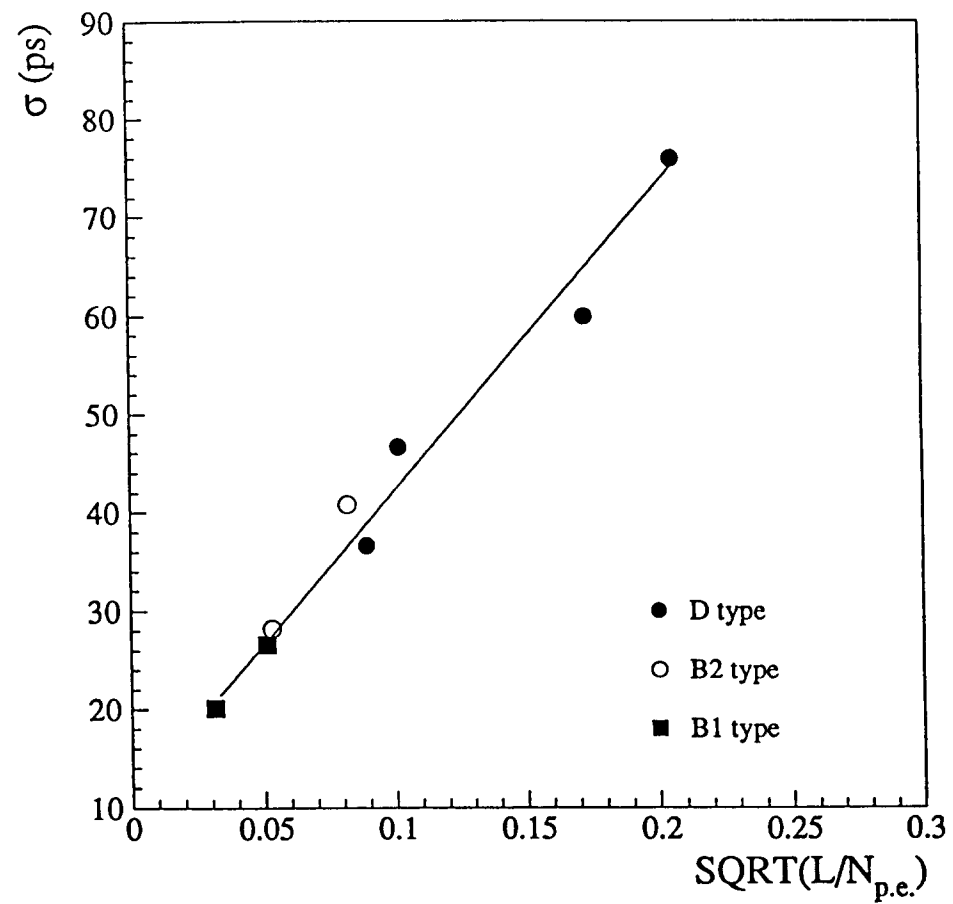


Fig. 8

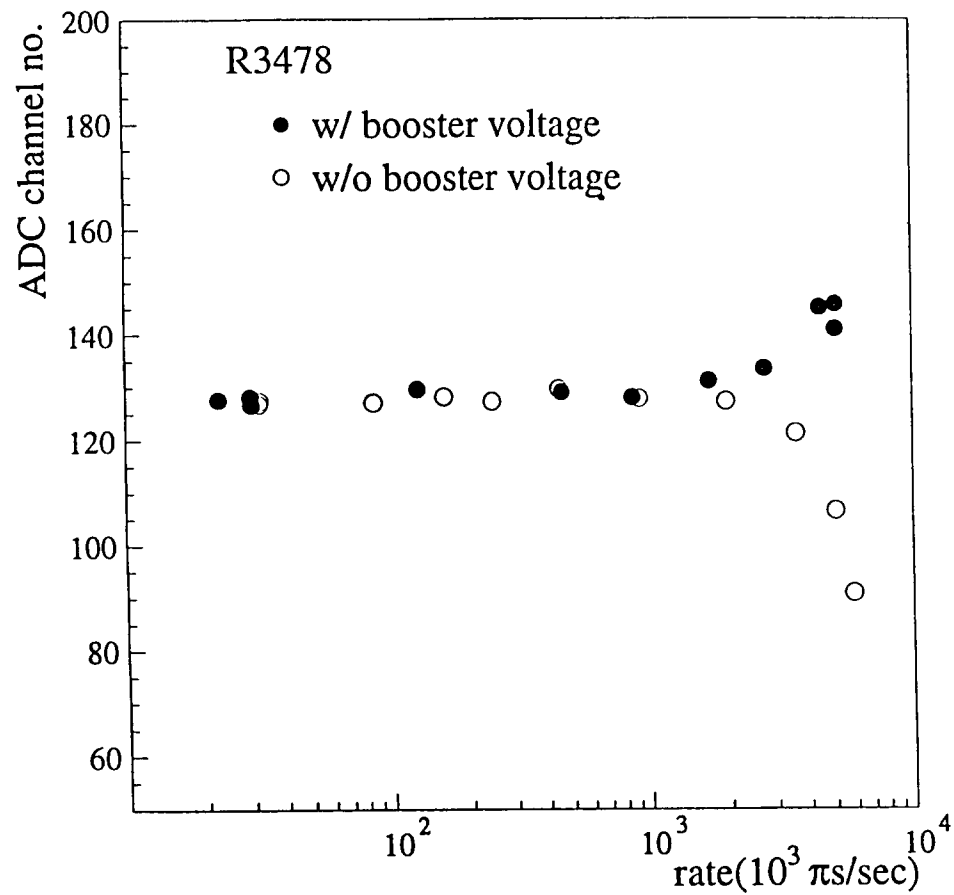


Fig. 9

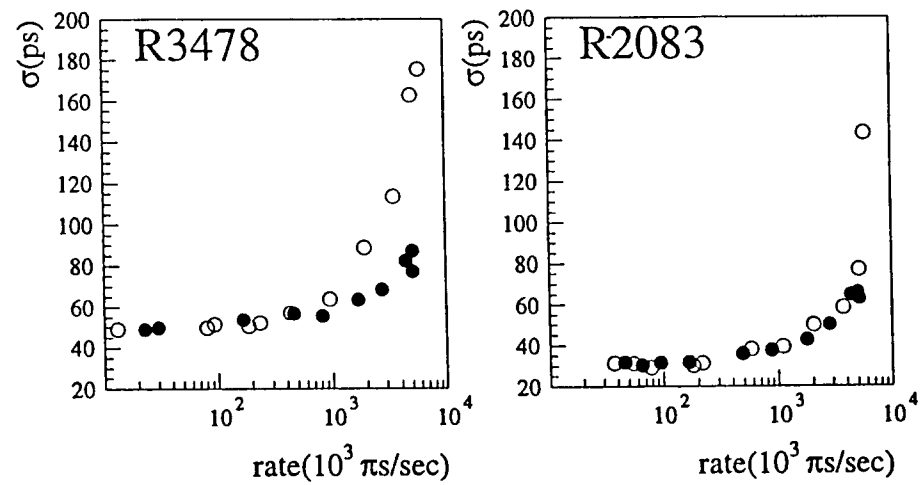


Fig. 10

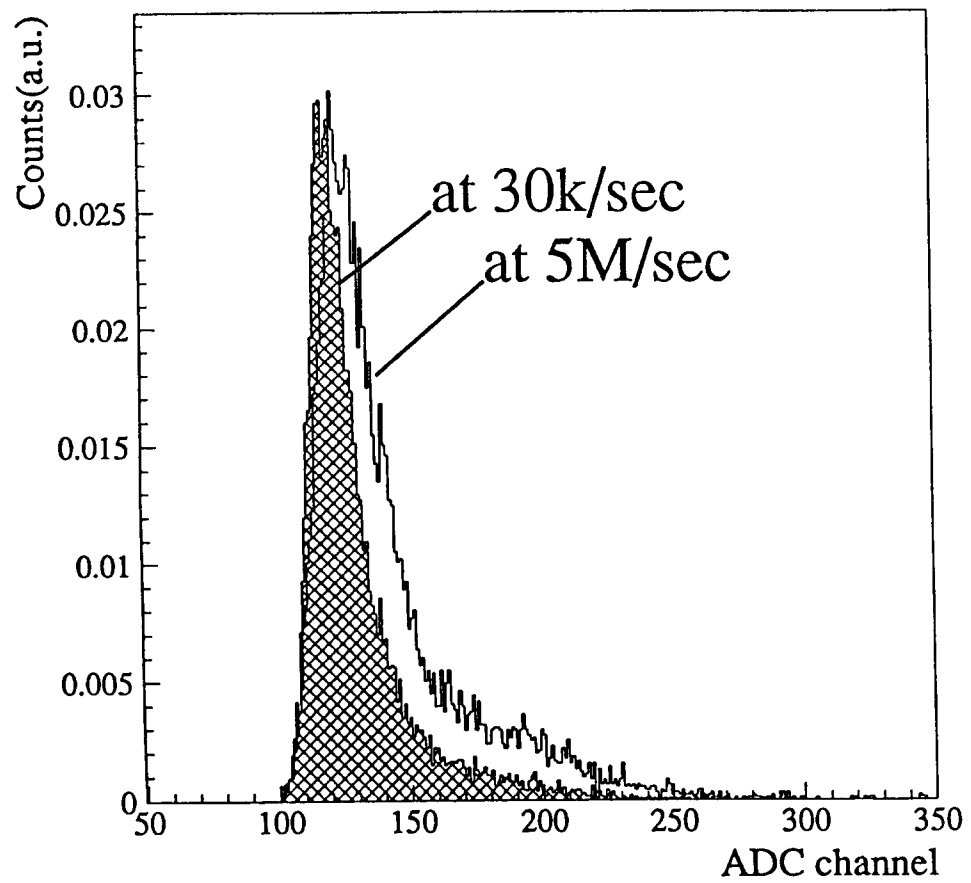


Fig. 11

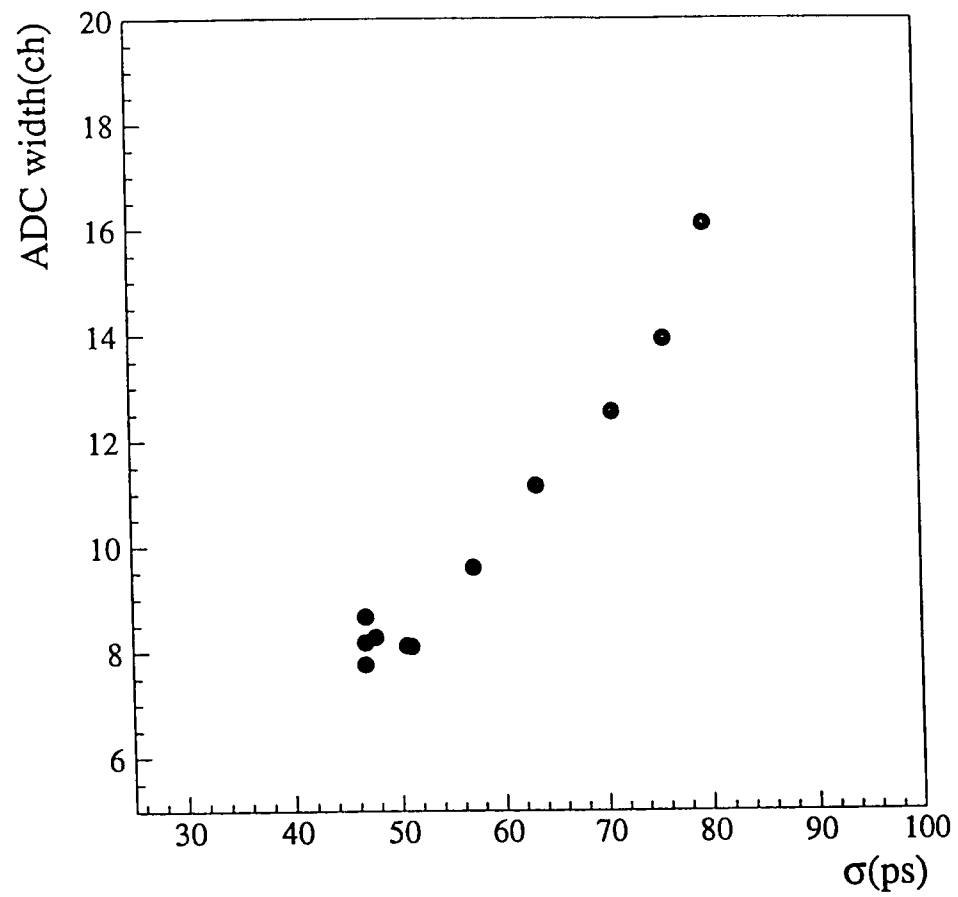


Fig. 12